10.1109/ULTSYM.2012.0586

Accuracy Of Backscatter Coefficient Estimation Using Highly Focused Transducers

Diego Panizo
and Roberto Lavarello
Laboratorio de Imágenes Médicas
Sección Electricidad y Electrónica
Pontificia Universidad Católica del Perú
San Miguel, Lima 32, Perú

Goutam Ghoshal
and Michael Oelze
Bioacoustics Research Laboratory
Department of Electrical and Computer Engineering
University of Illinois at Urbana-Champaign
Urbana, IL 61801

***Abstract*—Backscatter coefficients (BSCs) have been proposed for decades for tissue characterization. The availability of formulations based on weakly focusing conditions has resulted in a widespread use of large focal number (f/#) transducers for BSC estimation. The use of highly focused transducers (HFTs) offers the possibility of improving the spatial resolution of BSC-based imaging. The model by Chen et al. [1] was developed for estimating BSCs using transducers of arbitrary f/#. However, to this date only preliminary experimental validation of this method has been performed. The goal of the present study is to analyze for the first time the accuracy of Chen's method when estimating BSC vs. frequency curves with HFTs through both simulations and experiments.**

In simulations, BSC estimates were obtained using synthetic data produced with FIELD II, thereby including frequency-dependent diffraction effects, from a simulated phantom containing 41 μm diameter solid spheres. The bandwidths of the simulated transducers ranged from 6-21 MHz with f/#s between 1.5 and 3. In physical experiments, radio frequency (rf) data were obtained with 15 MHz, f/1.5 and 10 MHz, f/2 transducers from a physical phantom containing glass beads of 41+/-5 μm diameter. BSC estimates were produced using two methods: Chen's model (CM) and Chen's approximate model for weakly focusing conditions (CAM). Accuracy was quantified using the mean fractional error (MFE) between the estimated and theoretical BSC curves. BSCs were estimated using gate lengths (Δz) between 15λ and 30λ.

In simulations, the MFE using the CAM ranged from 30.6%-56.7%, 11.8%-32.3%, and 4.8%-9.3% for an f/1.5, f/2, and f/3 transducers, respectively. The MFEs were reduced to 8.5%-9.3%, 7%-7.4%, and 3.9%-4.1%, respectively when using the CM. In experiments, the MFE using the CAM ranged from 22.6%-43.3% and 6%-20.7% with the f/1.5 and f/2 transducers, respectively. The MFEs were reduced to 13.2%-26.7% and 5.9%-7.8% respectively when using the CM. These results suggest that significant improvements in the accuracy of BSC estimation with highly focused transducers can be achieved by using Chen's general model instead of weakly focused transducer formulations.

I. Introduction

In many tissue characterization applications it is desirable to obtain information about the microstructure of the material that is being analyzed. The backscatter coefficient (BSC) is an intrinsic property that quantifies the amount of energy that is reflected by a material as a function of the ultrasound wave frequency. Many studies suggest the usefulness of BSCs to derive properties of tissue microstructure. BSCs can be estimated using ultrasound transducers with different focal numbers. The use of highly focused transducers offers the possibility of improving the spatial resolution of BSC-based imaging by reducing the size of the region of interest (ROI) required to estimate BSCs.

In order to obtain meaningful information from BSCs it is necessary to compensate for the ultrasound system-dependent properties (transducer diffraction pattern, acoustic-electric response, etc). The availability of methods for estimating BSCs derived from weakly focusing conditions [1], [2] and the extended focal region that results from these conditions has resulted in an overwhelming number of studies that used weakly focused transducers to characterize hepatic [3], breast [4] and cardiac [5] tissues, among others. Nevertheless, highly focused transducers (i.e., focal number less than 2) have also been used for BSC estimation typically for high frequency applications [6], [7].

The work by Chen et al. [1] provides expressions to estimate BSCs using transducers with arbitrary focal number, and approximate expressions for the case of a weakly focused transducer. Therefore, the use of the models in [1] will allow to study the differences when estimating BSCs with and without assuming weakly focusing conditions from data obtained with highly focused transducers. Some studies available in the literature suggest that the general model in [1] may be used to compensate for the transducer diffraction pattern when estimating BSCs [8], [9]. However, a conclusive study on BSC estimation from properly characterized scattering media using highly focused transducers has not yet been conducted.

The goal of the present study is to analyze for the first time the accuracy of Chen's method when estimating BSC vs. frequency curves with highly focused transducers through both simulations and experiments.

II. Methods

A. BSC estimation methods

Let $\left\langle |S_1(k)|^2 \right\rangle$ represent the average spectrum of several radio frequency (rf) lines gated between depths $(F - \Delta z/2)$ and $(F + \Delta z/2)$ using a rectangular window, where F is

the transducer focal length and Δz is the length of the ROI. Backscatter coefficients $\eta(k)$ are estimated by removing system-dependent effects from $\left\langle |S_1(k)|^2 \right\rangle$. This is partially accomplished by dividing $\left\langle |S_1(k)|^2 \right\rangle$ with a reference spectrum $|S_2(k)|^2$ obtained from a suitable, well-characterized reflector. In addition, the diffraction of the ultrasonic transducer also has to be compensated.

Two methods for BSC estimation presented in [1], Chen's general model (CM) and its approximate version (CAM), are described in the following sections for simulated and experimental data.

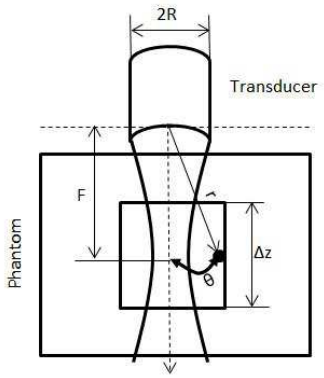

Fig. 1. Schematic diagram of the geometry.

1) Chen's model (CM) with a planar reference: In experiments, the reference spectrum $|S_2(k)|^2$ was obtained from a planar reflector with pressure reflection coefficient γ located at depth F. For this particular reference, BSCs can be estimated as (Ref [1], Eqs. (31), (34), (52) and (57))

$$\eta(k) = \frac{\left\langle |S_1(k)|^2 \right\rangle}{|S_2(k)|^2} \frac{\gamma^2}{A} D_2(G_P) H(k) \cdot \frac{1}{\xi(k)}. \tag{1}$$

$$D_2(G_P) = |\exp(-iG_P)[J_0(G_P) + iJ_1(G_P)] - 1|^2,$$

where A is the transducer area, $H(k)$ is a function that compensates for attenuation effects, $G_P = (kR^2/2F)$ is the pressure focusing gain of the transducer, R is the transducer radius, and $J_m(.)$ is the m-th order Bessel function. $\xi(k)$ is a diffraction correction function given by

$$\xi(k) = \int_{F-\frac{\Delta z}{2}}^{F+\frac{\Delta z}{2}} D_S(r;k)\mathrm{d}r, \tag{2}$$

$$D_s(r;k) = \frac{\pi a^2}{r^2} \int_{Z=0}^{Z=kR} 8 \left\{ [u_1(Y,Z)Z/Y]^2 + [u_2(Y,Z)Z/Y]^2 \right\}^2 Z^{-3} \left[1 - \left(\frac{Z}{kR} \right)^2 \right]^{-\frac{1}{2}} \mathrm{d}Z, \tag{3}$$

where $Z = kR\sin\theta$, $Y = (kR^2/r)(1 - r\cos\theta/F)$ (see Fig. 1 for definition of θ), and $u_1(Y,Z)$ and $u_2(Y,Z)$ are the Lommel function of the first and second order, given by

$$u_1(Y,Z) = \sum_{n=0}^{\infty} (-1)^n \left(\frac{Y}{Z} \right)^{2n+1} J_{2n+1}(Z),$$
$$u_2(Y,Z) = \sum_{n=0}^{\infty} (-1)^n \left(\frac{Y}{Z} \right)^{2n+2} J_{2n+2}(Z). \tag{4}$$

2) Chen's approximate model (CAM) with a planar reference: An approximate model to estimate BSCs using weakly focused transducers was also provided in [1]. For the particular case when the ROI is centered around F and for weakly focusing conditions, BSCs can be approximately estimated as (Ref [1], Eqs. (31), (54) and (57))

$$\eta(k) = \frac{\left\langle |S_1(k)|^2 \right\rangle}{|S_2(k)|^2} \frac{\gamma^2 F^2}{0.46 A \Delta z} D_2(G_P) H(k). \tag{5}$$

3) CM and CAM with a point reference: In simulations, BSC estimates were obtained using synthetic data produced with FIELD II [10], thereby including frequency-dependent diffraction effects. The use of a planar reflector as reference in FIELDII is not practical and therefore a point reference was used. The use of a different reference results in modifications to the equations presented in Sections II.A.1 and II.A.2. Specifically, the BSCs using the CM can be estimated as

$$\eta(k) = \frac{\left\langle |S_1(k)|^2 \right\rangle}{|S_2(k)|^2} \frac{A}{(2\pi)^2 F^4} \cdot \frac{1}{\xi(k)}, \tag{6}$$

and using the CAM as

$$\eta(k) = \frac{\left\langle |S_1(k)|^2 \right\rangle}{|S_2(k)|^2} \frac{A}{0.46(2\pi)^2 F^2 \Delta z}. \tag{7}$$

B. Simulated and experimental data

1) Simulated data: In simulations, BSC estimates were obtained from simulated phantoms containing 41 μm diameter solid spheres. Attenuation effects were not included. The properties of the simulated transducers are given in Table I.

TABLE I
TRANSDUCERS USED TO OBTAIN THE SIMULATED DATA

f_0	$f\#$	Diameter
10 MHz	2	1 in
13 MHz	3	0.5 in
15 MHz	1.5	0.5 in

2) Experimental data: In physical experiments, rf data were obtained from an agar physical phantom containing glass beads of 41+/-5 μm diameter. The attenuation coefficient was measured independently using an insertion loss technique in through transmission. The reference was a Plexiglass planar reflector ($\gamma = 0.37$). The properties of the simulated transducers are given in Table II.

TABLE II
TRANSDUCERS USED TO OBTAIN THE EXPERIMENTAL DATA

Experimental Transducers		
f_0	$f\#$	Diameter
10 MHz	2	1 in
15 MHz	1.5	0.5 in

C. Accuracy assessment

Accuracy was quantified using the mean fractional error (MFE) between the estimated $\eta(k)$ and theoretical $\eta_{th}(k)$ BSC curves as

$$\text{MFE} = \frac{1}{N}\sum_{i=1}^{N}\frac{|(\eta(k_i) - \eta_{th}(k_i))|}{\eta(k_i)} * 100, \tag{8}$$

The theoretical BSC was calculated using

$$\eta_{th} = \frac{\beta}{4\pi}\int_0^\infty p(a)\sigma(k,a)\mathrm{d}a, \tag{9}$$

where β is the concentration of scatterers per unit of volume, $p(a)$ is the estimated scatterer size probability distribution function estimated experimentally from optical microscopy images, and $\sigma(k,a)$ is the backscattering cross-section of an individual scatterer of radius a.

Both for simulated and experimental data, BSCs were estimated using gate lengths Δz between 15λ and 30λ. Variance effects were reduced by averaging data from 120 and 441 rf lines in simulations and experiments, respectively.

III. RESULTS

The MFE values obtained both for simulated and experimental data are reported in Table III for $\Delta z = 15\lambda$ and $\Delta z = 30\lambda$. The simulation results suggest that the CAM MFE increases with increasing Δz for a fixed f/# value, with MFEs exceeding 50% for the 10 MHz, f/1.5 transducer. This result is expected because the -6-dB focal depth of a focused circular piston is approximately $7\text{f/\#}^2\lambda$, and therefore diffraction effects across a given distance are more significant for lower f/# values. For example, for an f/1.5 transducer the focal depth is approximately 15.75λ and therefore the use of Δz values of 15λ or 30λ implies that the ROI covers the full extension of the focal region or further. In contrast, the use of the CM resulted in MFE values that were highly insensitive to Δz for all focal numbers considered in the simulations. Moreover, the MFEs were largely reduced when using the CM instead of the CAM, with values below 10% for all three simulated cases and more than a fourfold increase in accuracy observed both with the f/1.5 and f/2 transducers for $\Delta z = 30\lambda$.

The improvements in BSC estimation accuracy were much more evident when highly focused transducers were used, but the results with the simulated f/3 transducer suggest that CM may also provide minor improvements when using weakly focused transducers compared to methods based on weakly focusing approximations such as the CAM.

It can also be observed that although the experimental results support the significant reduction on MFE when using the CM instead of the CAM, the accuracy improvements were not as large as the ones obtained in simulations. Potential reasons for this discrepancy may include errors in modeling the transducer geometry, errors in the assumed theoretical BSC, and noise effects. Regardless, the results support advocating for the use of CM when estimating BSCs instead of the CAM for highly focused transducers.

Figure 2 shows the experimental BSC curves produced with the 15 MHz, f/1.5 and 10 MHz, f/2 transducers using the CM and the CAM for $\Delta z = 15\lambda$ and $\Delta z = 30\lambda$. It can be observed that all the estimated BSC curves are closer to the theoretical ones after using the appropriate correction (i.e., the CM), which is consistent with the MFE values reported in Table III.

Although the choice of large Δz values allowed to analyze the ability of both CM and CAM to correct for depth-dependent diffraction effects, the choice of gate lengths as large as 30λ is not consistent with the goal of constructing high resolution quantitative ultrasound images. Therefore, a similar analysis using shorter ROIs centered at several depths along the transducer focal region should be conducted.

IV. CONCLUSIONS

The presented results suggest that significant improvements in the accuracy of BSC estimation with highly focused transducers can be achieved by using the Chen's general model instead of weakly focused transducer formulations. This conclusion is supported by the MFE results in different magnitudes for all the transducers presented, both for simulations and experiments.

ACKNOWLEDGMENT

This work was supported by PUCP Grant DGI2010-0105.

REFERENCES

[1] X. Chen, D. Phillips, K. Schwarz, J. Mottley, and K. Parker, "The measurement of backscatter coefficient from a broadband pulse-echo system: a new formulation," *IEEE Transactions on Ultrasonics, Ferroelectrics and Frequency Control*, vol. 44, pp. 515 – 525, 1997.

[2] R. J. Lavarello, G. Ghoshal, and M. L. Oelze, "On the estimation of backscatter coefficients using single-element focused transducers," *Journal of the Acoustical Society of America*, vol. 129, pp. 2903–2911, 2011.

[3] Z. F. Lu, J. Zagzebski, and F. Lee, "Ultrasound backscatter and attenuation in human liver with diffuse disease," *Ultrasound in Medicine & Biology*, vol. 25, pp. 1047–1054, 1999.

[4] M. L. Oelze and J. F. Zachary, "Examination of cancer in mouse models using high-frequency quantitative ultrasound," *Ultrasound in Medicine & Biology*, vol. 32, pp. 1639 – 1648, 2006.

TABLE III
MFE IN SIMULATIONS AND EXPERIMENTS

MFE in Simulations				
Transducer	CAM ($\Delta z = 15\lambda$)	CAM ($\Delta z = 30\lambda$)	CM ($\Delta z = 15\lambda$)	CM ($\Delta z = 30\lambda$)
10 MHz f/2	11.8%	32.3%	7%	7.4%
13 MHz f/3	4.8%	9.3%	3.9%	4.1%
15 MHz f/1.5	30.6%	56.3%	8.5%	9.3%
MFE in Experiments				
Transducer	CAM ($\Delta z = 15\lambda$)	CAM ($\Delta z = 30\lambda$)	CM ($\Delta z = 15\lambda$)	CM ($\Delta z = 30\lambda$)
10 MHz f/2	6%	20.7%	5.8%	7.8%
15 MHz f/1.5	22.6%	43.3%	13.2%	26.7%

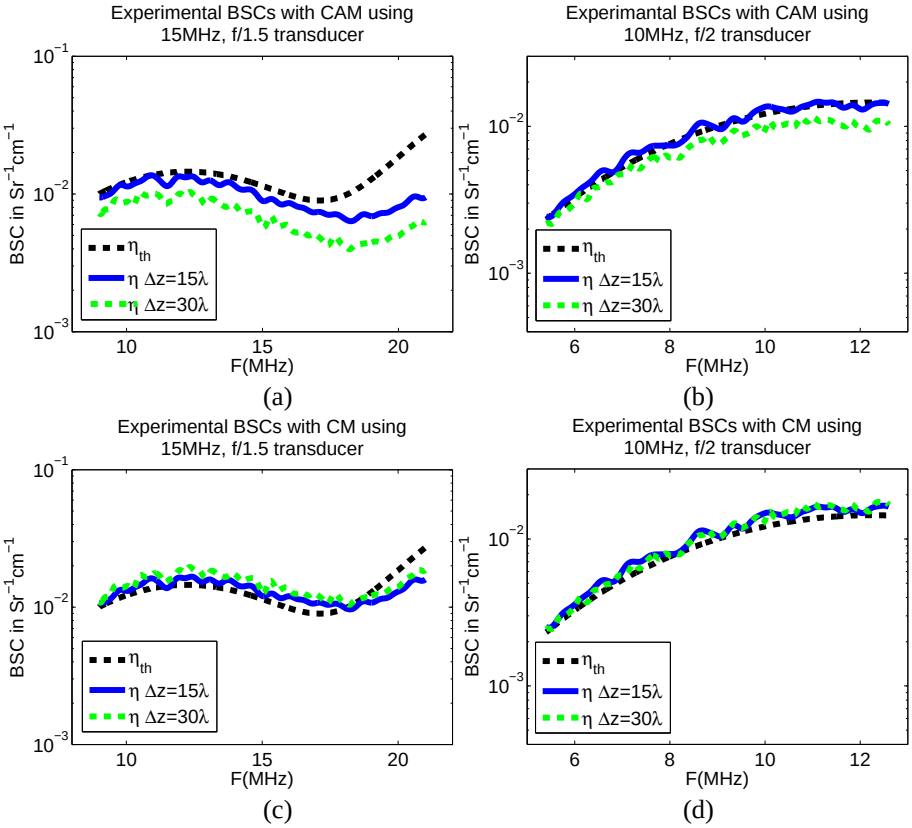

Fig. 2. BSCs estimates with fifteen and thirty wavelengths gated regions and theoretical BSCs (dotted line) for two experimental highly focused transducers ((a) and (c) corresponds to a transducer with f_0=15MHz, $F_\#$=1.5 and 0.5"diameter, (b) and (d) corresponds to a transducer with f_0=10MHz, $F_\#$=2 and 1"diameter). The first two estimates (top) were obtained using CAM and the second two (bottom) were obtained using CM.

[5] B. Barzilai, J. Saffitz, J. Miller, and B. Sobel, "Quantitative ultrasonic characterization of the nature of atherosclerotic plaques in human aorta," *Circulation Research*, vol. 60, pp. 459–463, 1987.

[6] M. Soldan, P. Silva, A. Schanaider, and J. Machado, "50 MHz ultrasound characterization of colitis on rats, in vitro," *Proceedings of the IEEE Ultrasonics Symposium*, pp. 1967 – 1970, 2008.

[7] F. Yu, E. Franceschini, B. Chayer, J. Armstrong, H. Meiselman, and G. Cloutier, "Ultrasonic parametric imaging of erythrocyte aggregation using the structure factor size estimator." *Biorheology*, pp. 343–363, 2009.

[8] J. Machado and F. Foster, "Experimental validation of a diffraction correction model for high frequency measurement of ultrasound backscatter coefficients," *Proceedings of the IEEE Ultrasonics Symposium*, vol. 2, pp. 1869 – 1872, 1998.

[9] B. I. Raju, K. J. Swindells, S. Gonzalez, and M. A. Srinivasan, "Quantitative ultrasonic methods for characterization of skin lesions in vivo," *Ultrasound in Medicine & Biology*, vol. 29, pp. 825 – 838, 2003.

[10] J. A. Jensen and N. B. Svendsen., "Calculation of pressure fields from arbitrarily shaped, apodized, and excited ultrasound transducers." *IEEE Transactions on Ultrasonics, Ferroelectrics and Frequency Control*, pp. 262–267, 1992.